Electronic Supplementary Information (ESI)

Polymorphism in 9,9-diarylfluorene-based organic semiconductors: influence on optoelectronic functions

Jun Yun Kim,[a] Takuma Yasuda,*[a,b,c] Yu Seok Yang,[a] Naoki Matsumoto[d] and Chihaya Adachi*[a,b]

[a] Department of Applied Chemistry, Graduate School of Engineering, and Center for Organic Photonics and Electronics Research (OPERA), Kyushu University, Japan

[b] International Institute for Carbon Neutral Energy Research (WPI-I2CNER), Kyushu University, Japan

[c] PRESTO, Japan Science and Technology Agency (JST), Japan

[d] Tosoh Corp., Nanyo Research Laboratory, Japan

E-mail: yasuda@cstf.kyushu-u.ac.jp; adachi@cstf.kyushu-u.ac.jp

Table of Contents:

General. ^{1}H and ^{13}C NMR spectra were recorded on a Bruker Avance III 500 spectrometer. Chemical shifts of ^{1}H and ^{13}C NMR signals were quoted to tetramethylsilane (δ = 0.00) and $CDCl_3$ (δ = 77.0) as internal standards. Matrix-assisted laser desorption ionization time-of-flight (MALDI-TOF) mass spectra were collected on a Bruker Daltonics Autoflex III spectrometer using dithranol as the matrix. Elemental analyses were carried out with a Yanaco MT-5 CHN corder. UV/Vis absorption and photoluminescence (PL) spectra were measured with a Shimadzu UV-2550 spectrometer and a Horiba Fluoromax-4 spectrophotometer, respectively. PL quantum yields were measured using an integration sphere system coupled with a photonic multichannel analyzer (Hamamatsu Photonics C9920-02, PMA-11). The HOMO energy levels were determined using a Riken-Keiki AC-3 ultraviolet photoelectron spectrometer. X-ray diffraction (XRD) patterns were obtained using a Rigaku Ultima IV diffractometer with Cu*K*α radiation. Thermogravimetric analysis (TGA) and differential scanning calorimetry (DSC) measurements were performed on a Shimadzu DTG-60AH at a scanning rate of 10 °C min^{-1} and a Netzsch DSC204 Phoenix calorimeter at a scanning rate of 5 °C min^{-1}, respectively, under N_2 atmosphere. AFM was performed using a JEOL JSPM-5400 scanning probe microscope with tapping-mode in air. X-ray crystallographic analysis was made on a Rigaku VariMax with a Saturn 724+ system with graphite monochromated Mo*K*α radiation. The structures were solved by direct methods (SIR2008)[1] and refined by full-matrix least-square techniques based on F^2 (SHELXL-97).[2]

Variable-angle spectroscopic ellipsometry (VASE). Thin films for the ellipsometry measurements were deposited onto Si (100) substrates, which were precleaned by detergent and organic solvents. VASE was performed using a fast spectroscopic ellipsometer (M-2000U, J. A. Woollam Co. Inc.). Seven different angles of the incident light from 45° to 75° with steps of 5° were used. At each angle, the experimental ellipsometric parameters Ψ and Δ were obtained simultaneously in 1.6-nm steps from 245 to 1000 nm. The VASE data were analyzed using WVASE32 software.

Amplified spontaneous emission (ASE) measurements. Thin films of **SFPT** and **BFPT** (thickness = 100 nm) were deposited on glass substrates. The films were optically pumped using a N_2 gas laser (MNL200, Laser Technik) at a wavelength of 337 nm with a pulse width of 500 ps and a repetition rate of 20 Hz. The ASE measurements were conducted by focusing the excitation light with an irradiation area of 400 μm × 10 mm. A detector (PMA-11, Hamamatsu Photonics) to observe the photoluminescence spectra was located on the edge of the films.

OFET device fabrication and measurements. **SFPT** and **BFPT** were incorporated into OFETs with a bottom-gate and top-contact geometry. For all of the OFET devices, heavily doped *n*-type Si wafers with a thermally grown 300-nm-thick SiO_2 layer were used as substrates. The SiO_2/Si substrates were pretreated with a piranha solution at 90 °C for 0.5 h, and then copiously cleaned by sonication in deionized water, acetone, and isopropanol in that order. The SiO_2/Si surface was treated with a self-assembled monolayer of hexamethyldisilazane (HMDS) by thermal evaporation for 1 h in air. The organic semiconductor layer of **SFPT** and **BFPT** was thermally evaporated on the substrates under high vacuum conditions. The devices were completed by evaporating gold (thickness = 50 nm) through a shadow mask to define the source and drain electrodes with a channel length of 20–100 μm on top of the organic layer. The output and transfer characteristics of the OFETs were measured using an Agilent B1500A semiconductor parameter analyzer under ambient conditions at room temperature. Field-effect mobilities (μ_{FET}) of the OFET devices were calculated in the saturation regime using the following equation: $I_D = (W/2L)\mu_{FET} C_i(V_G - V_{th})^2$, where I_D is the source–drain current, W and L are channel width and length, respectively, C_i is the capacitance per unit area of the gate dielectric (11 nF/cm^2), V_G is the gate voltage, and V_{th} is the threshold voltage.

Materials and syntheses. Commercially available reagents and solvents were used without further purification unless otherwise noted. All of the reactions were performed under an N_2 atmosphere in dry solvents. The synthetic routes for **SFPT** and **BFPT** are outlined in Scheme S1. 2,7-Dibromo-9,9'-spirobifluorene (**1**) and 2,7-dibromofluorenone (**2**) were purchased from TCI.

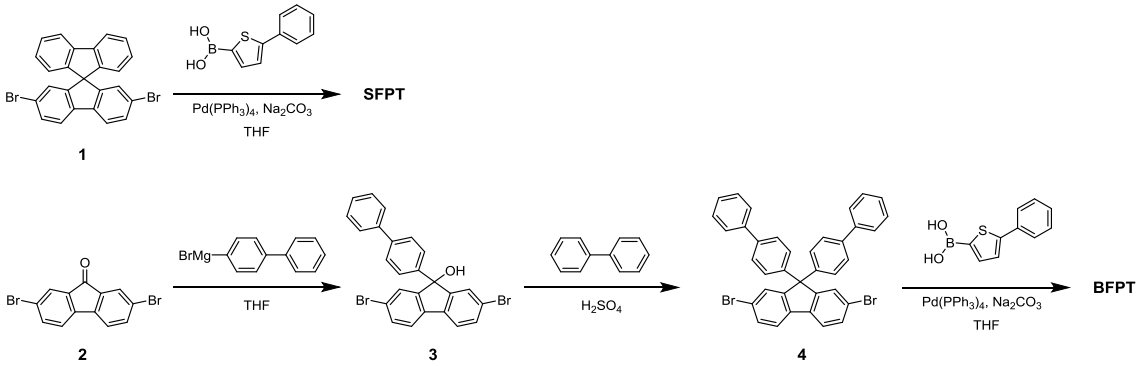

Scheme S1. Synthesis of **SFPT** and **BFPT**.

Synthesis of SFPT. To a mixture of **1** (2.00 g, 4.2 mmol) and 2-phenylthiophen-5-yl-boronic acid (1.82 g, 11.2 mmol) in dry THF (40 mL) were added $Pd(PPh_3)_4$ (0.30 g, 0.26 mmol) and aqueous Na_2CO_3 (2.0 M, 15 mL; Ar bubbled before use). The mixture was vigorously stirred under reflux for 48 h. After cooling to room temperature, the formed precipitate was collected by filtration and then washed with water and ethanol. The product was recrystallized from THF/methanol, and dried under vacuum to afford **SFPT** as a yellow solid (yield = 1.50 g, 56%). This compound was further purified by repetitive temperature-gradient sublimation before use. ^{1}H NMR (500 MHz, $CDCl_3$): δ 7.90 (d, J = 8.0 Hz, 2H), 7.84 (d, J = 8.0 Hz, 2H), 7.65 (dd, J = 7.5 Hz, 1.5 Hz, 2H), 7.54 (dd, J = 7.5 Hz, 1.0 Hz, 4H), 7.41 (d, J = 7.5 Hz, 2H), 7.33 (t, J = 7.5 Hz, 4H), 7.24 (t, J = 7.0 Hz, 2H), 7.16 (d, J = 4.0 Hz, 2H), 7.14 (t, J = 7.0 Hz, 2H), 7.11 (d, J = 4.0 Hz, 2H), 6.94 (d, J = 1.5 Hz, 2H), 6.82 (d, J = 7.5 Hz, 2H). ^{13}C NMR (125 MHz, $CDCl_3$): δ 149.97, 148.30, 143.50, 143.46, 141.82, 140.72, 134.22, 134.05, 128.85, 128.04, 127.93, 127.44, 125.61, 125.54, 124.26, 124.14, 123.85, 120.94, 120.44, 120.14, 65.99. MS (MALDI-TOF): m/z 633.37 $[M+H]^+$. Anal. calcd (%) for $C_{45}H_{28}S_2$: C 85.41, H 4.46; found: C 85.51, H 4.34.

Synthesis of 2,7-dibromo-9-biphenyl-9-hydroxyfluorene (3). 4-Biphenyl magnesium bromide was prepared from magnesium powders (694 mg, 28.6 mmol) 4-bromobiphenyl (6.15 g, 26.4 mmol) in dry THF (40 mL). The obtained Grignard solution was diluted with dry THF (50 ml), and **2** (7.51 g, 22.0 mmol) was then added into the solution. The mixture was refluxed for 5 h. After cooling to room temperature, the reaction mixture was quenched with an aqueous NH_4Cl solution (10%). The organic layer was washed with brine and dried over anhydrous $MgSO_4$. After filtration

and evaporation, the crude product was recrystallized from toluene to give **3** as pale yellow crystals (yield = 7.60 g, 70%). ^{1}H NMR (500 MHz, $CDCl_3$): δ 7.32-7.57 (m, 15H), 2.49 (s, 1H). ^{13}C NMR (125 MHz, $CDCl_3$): δ 151.82, 140.64, 140.51, 137.48, 132.45, 128.72, 128.39, 127.31, 127.26, 127.04, 125.66, 122.52, 121.53, 83.21.

Synthesis of 2,7-dibromo-9,9-bis(biphenyl)fluorene (4). To a mixture of **3** (1.60 g, 3.2 mmol), biphenyl (4.92 g, 32 mmol), and acetic acid (15 g) were added dropwise H_2SO_4 (0.94 g, 9.6 mmol) at room temperature. The mixture was stirred for 3 h at 80 °C. After cooling to room temperature, the reaction mixture was poured into a large amount of water. The formed precipitate was collected by filtration, washed with water and ethanol, and recrystallized from ethanol/THF to yield **4** as colorless crystals (1.20 g, 62%). ^{1}H NMR (500 MHz, $CDCl_3$): δ 7.23-7.63 (m, 24H). ^{13}C NMR (125 MHz, $CDCl_3$): δ 152.84, 143.22, 140.41, 140.05, 138.03, 131.08, 129.45, 128.77, 128.31, 127.35, 127.24, 126.90, 121.92, 121.67, 65.25.

Synthesis of BFPT. This compound was prepared in a fashion similar to **SFPT**, using **4** (2.00 g, 3.2 mmol), 2-phenylthiophen-5-yl-boronic acid (1.82 g, 8.9 mmol), and $Pd(PPh_3)_4$ (0.25 g, 0.22 mmol). The product was obtained as a yellow solid (yield = 1.60 g, 64%). This compound was further purified by repetitive temperature-gradient sublimation before use. ^{1}H NMR (500 MHz, $CDCl_3$): δ 7.79 (d, J = 8.0 Hz, 2H), 7.72 (d, J = 1.5 Hz, 2H), 7.68 (dd, J = 8.0 Hz, 1.5 Hz, 2H), 7.61 (dd, J = 8.0 Hz, 2.0 Hz, 4H), 7.56 (dd, J = 8.0 Hz, 2.0 Hz, 4H), 7.52 (dd, J = 8.0 Hz, 1.5 Hz, 4H), 7.25-7.42 (m, 26H). ^{13}C NMR (125 MHz, $CDCl_3$): δ 145.69, 144.06, 143.84, 143.66, 140.73, 140.41, 137.67, 132.05, 131.40, 131.37, 131.34, 127.62, 127.59, 127.57, 126.40, 126.33, 126.27, 125.34, 122.45, 65.19. MS (MALDI-TOF): m/z 787.75 $[M+H]^+$. Anal. calcd (%) for $C_{57}H_{38}S_2$: C 86.99, H 4.87; found: C 87.02, H 4.73.

References

1 M. C. Burla, R. Caliandro, M. Camalli, B. Carrozzini, G. L. Cascarano, L. De Caro, C. Giacovazzo, G. Polidori, D. Siliqi, and R. Spagna, *J. Appl. Cryst.*, 2007, **40**, 609.

2 G. M. Sheldrick, *Programs for Crystal Structure Analyses (Release 97-2)*, University of Göttingen, Germany, 1997.

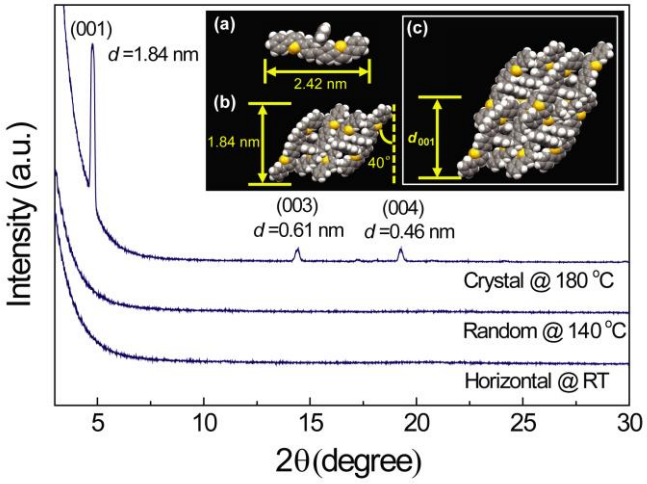

Fig. S1 XRD patterns of **SFPT** films in *a*-phase (bottom), *b*-phase (middle), and *c*-phase (top). Insets show (a) molecular length, (b) interlayer distance (1.84 nm) and tilted molecular orientation with respect to the substrate normal, calculated from XRD and X-ray crystallography data, and (c) crystal packing structure of **SFPT**.

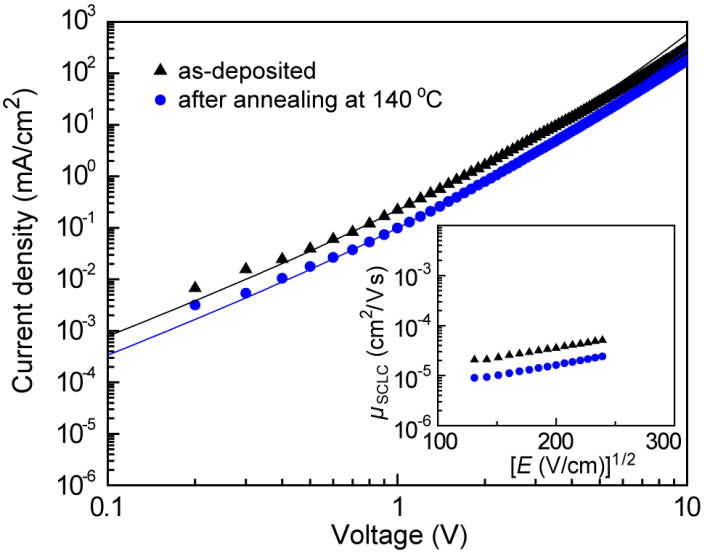

Fig. S2 Double logarithmic plots of *J*–*V* characteristics of hole-only devices comprising ITO/MoO_3 (0.8 nm)/**BFPT** (300 nm)/MoO_3 (10 nm)/Al (70 nm). The solid lines represent the best fits to the SCLC model. The inset shows the electric-field dependence of hole mobility (μ_{SCLC}) for the **BFPT** films before and after thermal treatment at 140 °C for 10 min.

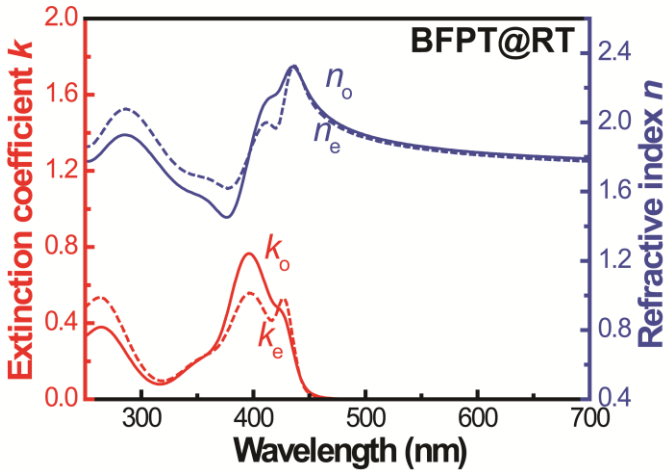

Fig. S3 Ordinary (solid lines) and extraordinary (dashed lines) extinction coefficients (k_o and k_e) and refractive indices (n_o and n_e) determined by VASE measurements for an as-deposited **BFPT** film.

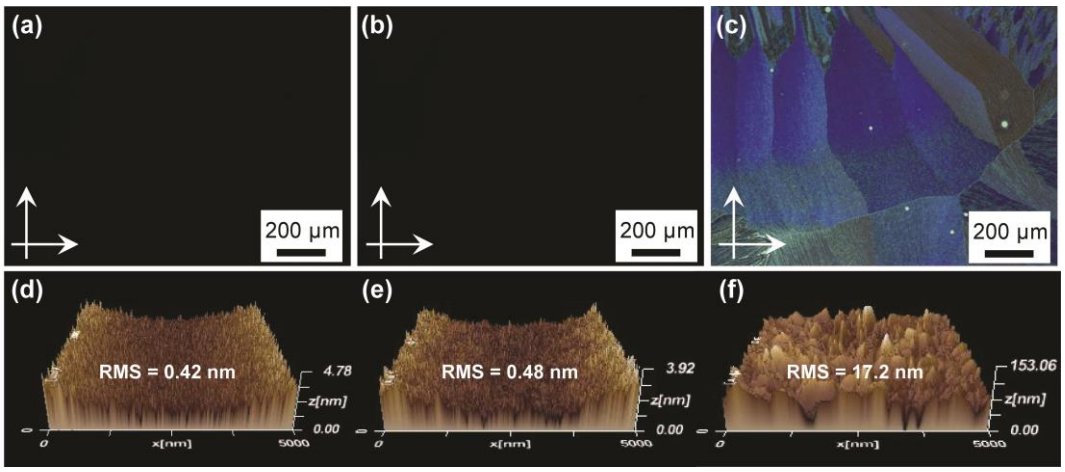

Fig. S4 POM (top panels) and AFM images (bottom panels) of **SFPT** films on Si/SiO_2 substrates: (a,d) at room temperature (*a*-phase) and after thermal treatment at (b,e) 140 °C (*b*-phase) and (c,f) 180 °C for 10 min (*c*-phase).

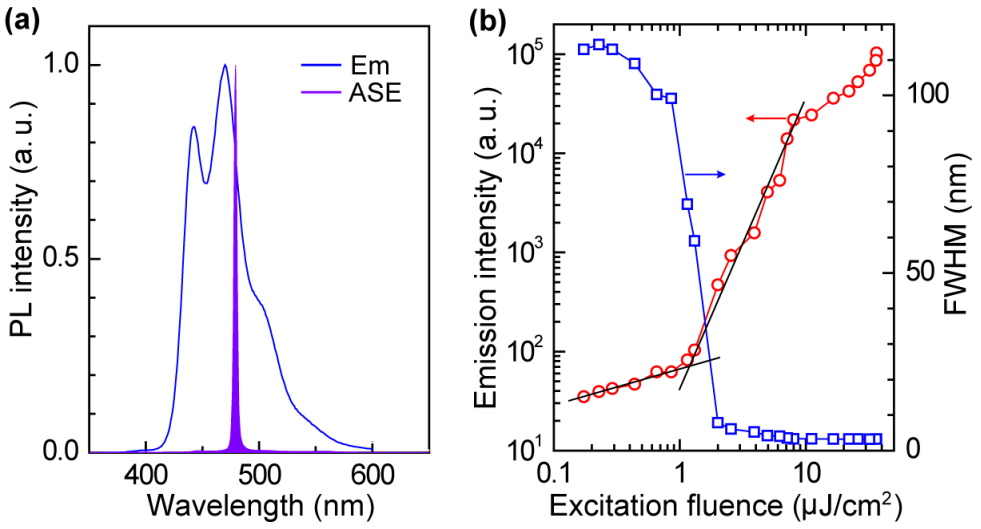

Fig. S5 (a) PL emission and ASE spectra of a 100-nm-thick **SFPT** film in the *b*-phase after thermal annealing at 140 °C for 10 min. (b) Emission intensity and full width at half-maximum (FWHM) of PL as a function of excitation fluence.

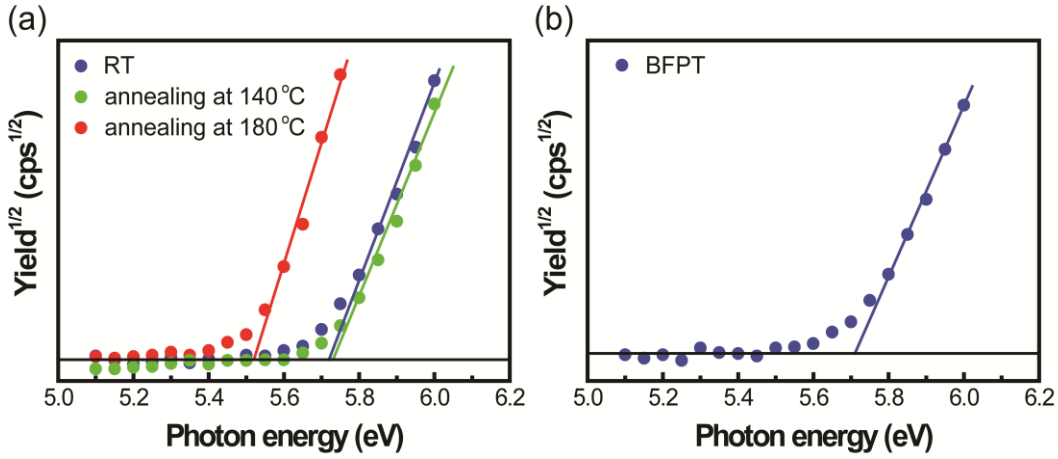

Fig. S6 Photoelectron yield spectra of (a) **SFPT** and (b) **BFPT**.

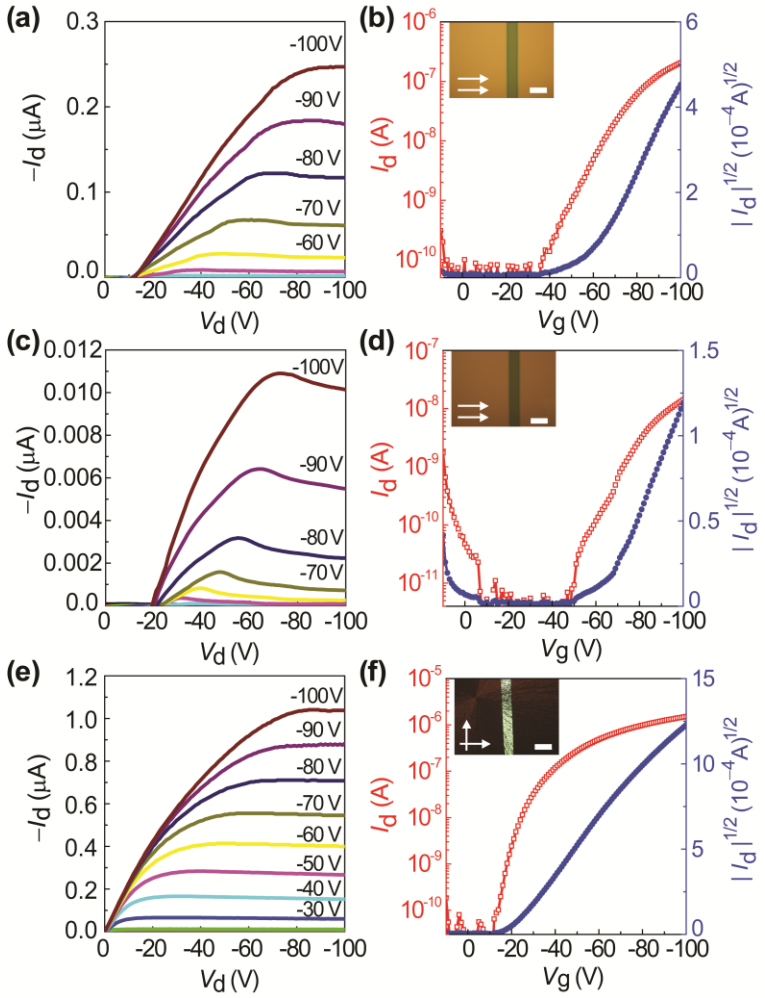

Fig. S7 Output (left panels) and transfer characteristics (right panels) of OFETs based on **SFPT** films in (a,b) *a*-phase, (c,d) *b*-phase, and (e,f) *c*-phase. The insets show the optical microscopic images of the devices (scale bar = 100 μm).

Table S1 Summary of OFET properties of **SFPT**

polymorph	orientation	μ_{FET} (cm^2/Vs)	V_{th} [a)] (V)	I_{on}/I_{off} [b)]
a-phase	horizontal	1.2×10^{-3}	−57	10^4
b-phase	random	1.1×10^{-4}	−64	10^4
c-phase	crystalline	3.7×10^{-3}	−20	10^5

[a)] Threshold voltage was determined by extrapolating the $|I_D|^{1/2}$ vs V_G plot to $I_D = 0$

[b)] On/off ratio was determined from the I_D at $V_G = 0$ V (I_{off}) and $V_G = -100$ V (I_{on}).